



NRC Publications Archive Archives des publications du CNRC

Assessment of concrete slab quality and layering by guided and surface wave testing

Al Wardany, R.; Ballivy, G.; Gallias, J-L.; Saleh, K.; Rhazi, J.

This publication could be one of several versions: author's original, accepted manuscript or the publisher's version. /
La version de cette publication peut être l'une des suivantes : la version prépublication de l'auteur, la version acceptée du manuscrit ou la version de l'éditeur.

Publisher's version / Version de l'éditeur:

ACI Materials Journal, 104, May/June 3, pp. 268-275, 2007-05-01

NRC Publications Record / Notice d'Archives des publications de CNRC:

<https://nrc-publications.canada.ca/eng/view/object/?id=436aa4d6-b5e1-4286-89e7-cba175d28e2>;
<https://publications-cnrc.canada.ca/fra/voir/objet/?id=436aa4d6-b5e1-4286-89e7-cba175d28e23>

Access and use of this website and the material on it are subject to the Terms and Conditions set forth at

<https://nrc-publications.canada.ca/eng/copyright>

READ THESE TERMS AND CONDITIONS CAREFULLY BEFORE USING THIS WEBSITE.

L'accès à ce site Web et l'utilisation de son contenu sont assujettis aux conditions présentées dans le site

<https://publications-cnrc.canada.ca/fra/droits>

LISEZ CES CONDITIONS ATTENTIVEMENT AVANT D'UTILISER CE SITE WEB.

Questions? Contact the NRC Publications Archive team at

PublicationsArchive-ArchivesPublications@nrc-cnrc.gc.ca. If you wish to email the authors directly, please see the first page of the publication for their contact information.

Vous avez des questions? Nous pouvons vous aider. Pour communiquer directement avec un auteur, consultez la première page de la revue dans laquelle son article a été publié afin de trouver ses coordonnées. Si vous n'arrivez pas à les repérer, communiquez avec nous à PublicationsArchive-ArchivesPublications@nrc-cnrc.gc.ca.





<http://irc.nrc-cnrc.gc.ca>

Assessment of concrete slab quality and layering by guided and surface wave testing

NRCC-49273

Al Wardany, R., Ballivy, G., Gallias, J-L.,
Saleh, K., Rhazi, J.

May 1, 2007

A version of this document is published in / Une version de ce document se trouve dans:
ACI Materials Journal, 104, (3), May/June, pp. 268-275

The material in this document is covered by the provisions of the Copyright Act, by Canadian laws, policies, regulations and international agreements. Such provisions serve to identify the information source and, in specific instances, to prohibit reproduction of materials without written permission. For more information visit <http://laws.justice.gc.ca/en/showtdm/cs/C-42>

Les renseignements dans ce document sont protégés par la Loi sur le droit d'auteur, par les lois, les politiques et les règlements du Canada et des accords internationaux. Ces dispositions permettent d'identifier la source de l'information et, dans certains cas, d'interdire la copie de documents sans permission écrite. Pour obtenir de plus amples renseignements : <http://lois.justice.gc.ca/fr/showtdm/cs/C-42>



National Research
Council Canada

Conseil national
de recherches Canada

Canada

ASSESSMENT OF CONCRETE SLAB QUALITY AND LAYERING BY GUIDED AND SURFACE WAVE TESTING

Riad Al Wardany, Gerard Ballivy, Jean-Louis Gallias, Kaveh Saleh and Jamal Rhazi

Biography: Riad Al Wardany, civil engineer (Beirut, Lebanon, 2000). He is currently a research officer at the National Research Council Canada, Centre for Sustainable Infrastructure Research. He received his PhD in civil engineering from the University of Sherbrooke and the University of Cergy-Pontoise, France, in 2005; and his MSc in civil engineering materials and structures from the University of Toulouse III, France in 2001. His research interests include nondestructive testing of concrete structures.

Gerard Ballivy, geological engineer (Nancy, France, 1964). He is specialized in applied geotechnology at the University of Grenoble and “École Polytechnique de Montréal”. In 1977, after twelve years with Hydro-Québec and the City of Montreal, he joined the University of Sherbrooke as a professor where he established the Laboratory of Rock Mechanics and Applied Geology. Instrumentation, environment, waste stabilization management and non-destructive methods are his main areas of interest and research. He is holder of the NSERC-Industry Research Chair on Concrete NDT and Instrumentation, which focuses on nondestructive testing of concrete.

Jean-Louis Gallias, civil engineer (NTUA, Athens, Greece, 1978). He is specialized in physico-chemical properties of cement-based materials at Paul Sabatier University, Toulouse, France. He is professor in the department of civil engineering at the University of Cergy-Pontoise, France, since 1994. His main research interests include the microstructure of cementitious materials in relation to physical and mechanical performance and durability parameters.

Kaveh Saleh, civil engineer from Tehran University (1978). He obtained his MSc in soil mechanics (1982) and his PhD in rock mechanics from “École Centrale de Paris” (1985). He worked as researcher in the Research Center of the French Petroleum Company (TOTAL-France) until 1988, after which he joined the University of Sherbrooke. Since 1992, Dr. Saleh has been in charge of civil engineering research projects at the Research Institute of Hydro-Québec (IREQ) and he also holds the position of adjunct professor at the University of Sherbrooke. His areas of interest are instrumentation, diagnostic and refection of structures, particularly for concrete dams.

Jamal Rhazi, adjunct professor in the department of civil engineering at the University of Sherbrooke. His research interests include instrumentation and nondestructive testing of concrete structures.

ABSTRACT

This paper presents an experimental study on the investigation of concrete properties by guided and surface wave nondestructive testing. Applications were made on two large slabs simulating homogeneity and layering in concrete, respectively. An efficient non-intrusive method was used to evaluate the concrete quality by solving the modal propagation problem of Lamb guided waves and Rayleigh surface waves. Lamb waves were used to determine the Poisson's ratio and the Young's modulus of the concrete slabs. Rayleigh waves were identified using Lamb wave fundamental-modes; thereafter, the inverse problem of Rayleigh waves was solved to evaluate the variation of shear wave velocity with depth and thus characterize the layered slab. The obtained results demonstrate the high potential of this tool that can easily be used for insitu assessment of concrete structures.

Keywords: concrete slabs; layering; nondestructive testing; Rayleigh wave; Lamb wave, frequency-wavenumber analysis.

INTRODUCTION

Near-surface damage is a common problem for most concrete structures exposed to severe environmental conditions such as the freeze-thaw cycles. The repair process requires good assessment of the concrete quality, and proper investigation of the depth of near-surface degradation. Evaluating these elements by retrieving cores from the concrete structure represents a destructive approach, which is often expensive and illustrates only local characteristics of concrete. In order to nondestructively provide the required information on concrete conditions, several methods such as ultrasonic pulse velocity, ultrasonic echo, impact echo and ground-penetrating radar are used in civil engineering^{1,2}. However, these methods have their own limitations in determining the concrete stiffness profile (quality versus depth). Thus, several research studies have focused, over the last few years, on the use of the Spectral Analysis of Surface Waves method (*SASW*), which was initially developed to characterize stratified media such as soils and pavements^{3,4}. The advantage of the *SASW* method is its ability to investigate elastic properties of solid media with depth using a simple test setup applied at the free surface of the solid half-space. The *SASW* test is based on the generation of a transient stress pulse by a mechanical impact at the surface of the tested medium. Two receivers are positioned at the same surface to measure the propagation of Rayleigh surface waves. Depending on the impact duration, Rayleigh waves with various wavelengths (frequencies) are produced. The shorter wavelengths (higher frequencies) propagate in the near surface layers, while the longer wavelengths (lower frequencies) penetrate more deeply into the medium. The phase velocity of a given wavelength (frequency) depends on the mass density and the elastic properties (shear modulus and Poisson's ratio) of the layers traveled by the wave. The *SASW* data analysis consists of evaluating the phase velocity of Rayleigh waves for all generated wavelengths (frequencies) from the unwrapped phase between the signals acquired at the two receivers. The obtained curve (phase velocity versus wavelength or

frequency) is called “dispersion curve” and it is assumed to represent the fundamental-mode of Rayleigh waves. The “dispersion” illustrates the phenomenon that the different wavelengths (frequencies) traveling the medium have different phase velocities. The shear modulus profile of the tested medium is determined by solving the inverse problem of Rayleigh waves using the calculated dispersion curve. During inversion, the solid is modeled as a system of horizontal layers with equal thicknesses; each layer is affected by a mass density, a Poisson’s ratio and a shear wave velocity. The theoretical dispersion curve is calculated for the assumed model using Rayleigh wave theory and then compared to the measured dispersion curve. If the relative difference between the compared phase velocities is significant (greater than a user defined percentage), the model is adjusted and a new profile is assumed. When the experimental curve and the theoretical curve become sufficiently close, the solution converges and the assumed model in the last iteration is considered to be representative of the tested medium. More details about the inversion process can be found in Rix and Leipski⁵.

The transfer of the *SASW* method to concrete structures was not so obvious; the results reported in the few studies carried out on structural elements seem to be not sufficiently reliable. Previous applications on concrete slabs showed fluctuations of the dispersion curve and significant errors in the estimation of the concrete stiffness profile^{6,7}. It is important to note that in those studies, the elastic waves propagating at the surface of concrete slabs were always interpreted as Rayleigh waves^{8,9,10}. However, the finite dimensions of concrete slabs generate another type of elastic waves called Lamb waves, which are very energetic and dominate the vibrations produced at the surface¹¹. Furthermore, Lamb waves propagate with different modes that can contribute significantly in the *SASW* test at the same time. This modal phenomenon is the main cause of ambiguity of the *SASW* results, due to the fact that modal analysis is not implemented in the signal-processing algorithm of the method. Recent studies

in the geotechnical field revealed similar limitations of the *SASW* method attributed to the participation of Rayleigh wave higher order modes in the test^{12,13}. In order to overcome the weakness of the *SASW* method, a method, named *FK*, has been proposed in this study. The method resolves fundamental and higher order modes of both Lamb and Rayleigh waves to accurately evaluate concrete slab quality with depth.

RESEARCH SIGNIFICANCE

The investigation of concrete properties by the dispersion analysis of elastic waves propagating at the surface of concrete slabs requires a complete solving of the vibration modes of the slab; the traditional *SASW* method is not very efficient to resolve such a problem. This study examines the effectiveness of an alternative multi-sensor approach in solving the modal phenomenon of propagation of Lamb and Rayleigh waves in concrete slabs. The method involves an accurate strategy that allows identification of fundamental and higher order modes of Lamb and Rayleigh waves, and thus a good evaluation of concrete quality and layering.

GUIDED AND SURFACE WAVE TESTING

Elastic energy introduced by a mechanical impact into solid media such as concrete, propagates through hemispherical wavefronts called body waves. Body waves are of two kinds: “pressure waves” and “shear waves”. In solid plates, for example concrete slabs, guided waves known as “Lamb waves” are also created. At the free surface of a solid half-space, such as massive concrete structures, another type of elastic waves, called “surface waves” is formed. Surface waves propagate through cylindrical wavefronts; they are “Rayleigh waves” and “Love waves”. The formation of Rayleigh waves requires free boundary conditions only, while Love waves are produced under supplementary specific conditions of the stratified medium and the source.

Lamb Guided Waves

The most important type of guided waves is Lamb waves, which are elastic perturbations of the material particles guided by the two parallel surfaces of a plate¹⁴. Lamb waves are formed by interference of multiple reflections and refractions of body waves on the two surfaces of the plate. The particles are perturbed in the direction of the wave propagation and perpendicularly to the plate's surfaces. Lamb waves are dispersive, and their propagation in the plate is governed by an infinite number of modes (fundamental-modes and higher order modes) classified into two groups, symmetric and antisymmetric, which propagate independently. The phase velocity of a Lamb wave depends on the thickness, the Poisson's ratio of the plate and the frequency.

Rayleigh Surface Waves

Rayleigh surface waves are elastic perturbations that propagate along the air-solid interface¹⁵ of a solid medium. The material particles at the surface move in an elliptical path within the vertical plane containing the direction of the wave propagation. At the surface of a homogeneous half-space, Rayleigh waves occupy most of the total energy generated and the different wavelengths (frequencies) propagate with a constant phase velocity. The vibrations are governed by only a fundamental-mode where the amplitude of particle motion decreases exponentially with depth and becomes insignificant at a depth of approximately two wavelengths. The cylindrical wavefront shape gives Rayleigh waves low geometrical spreading relatively to the spherical wavefront shape of body waves; at a distance (r) from the source, the amplitude of Rayleigh waves is proportional to $(1/r^{0.5})$ whereas it is proportional to $(1/r^2)$ for body waves. This explains why Rayleigh wave amplitude is always larger than that of body waves at the surface. In a stratified half-space, Rayleigh waves are dispersive; the different wavelengths (frequencies) travel the layered system at different modal velocities

related to the elastic properties (Poisson's ratio, shear modulus) and the mass density of the traveled layers. In solid plates, Rayleigh waves are formed by the superposition of Lamb wave fundamental-modes for all waves having a wavelength less than approximately half the thickness of the slab¹⁶.

FK Method

The use of Lamb waves represents a promising approach for the global characterization of concrete slabs, while Rayleigh waves permit the assessment of concrete properties in terms of depth. Therefore, solving the modal propagation problem of Lamb and Rayleigh waves in concrete slabs leads to the investigation of the concrete quality and layering, respectively. Based on this principle, a method named *FK* (F = frequency, K = wavenumber) was constructed, tested and presented in this study. The method uses the frequency-wavenumber analysis to resolve the different modes of propagation of Rayleigh and Lamb waves; this approach has demonstrated accuracy in the dispersion analysis of surface waves in geotechnical and pavement applications^{17,18,19}. The *FK* test setup involves a series of Na accelerometers linearly positioned with equal spacing dx at the concrete surface to monitor the surface vibrations produced by the propagation of elastic waves (**Fig. 1**). Lamb and Rayleigh waves are generated by an impact source (steel ball, hammer) or a piezoelectric pulsar source placed at a distance d from the first accelerometer. An external trigger is used to start data acquisition at the same time as the impact. The acquired signals are amplified and recorded using a portable acquisition system. Thereafter, the source is moved away a certain distance $Na \times dx$ from its position and a second series of measurements is carried out. The same operation is repeated several times at Np positions of the source in order to gather a total number of $Na \times Np$ signals, called "seismogram". Data analysis of the collected seismogram consists of applying a Fast Fourier Transformation (FFT) along the time-axis to transfer data

from the time domain to the frequency domain. This allows spatial distribution of energy for all frequencies propagating along the whole length of the *FK* test. When it is applied evenly on the transformed data along the space-axis (distance), the FFT provides information on the wavenumber content of the seismogram, which is directly related to the propagating wavelengths. The result is a two dimensional representation of the energy of elastic waves captured at the concrete surface; it illustrates the seismogram content in terms of frequency and wavenumber. Knowing the relation between the phase velocity, the frequency f and the wavenumber k , $V_{ph} = \frac{2 \pi f}{k}$, the seismogram energy is redistributed in the frequency-phase velocity domain by a simple axis transformation. The obtained image is called an *FK* image, and it illustrates the different modes of propagation of Lamb and Rayleigh waves. The resolution of the *FK* image can be improved by extending the seismogram signals with zeros in the time and/or the space direction before applying the FFTs (zero padding). The dispersion curves are finally determined for the different modes by selecting the peaks of energy (crests) on the *FK* image.

After extracting the modes of Lamb and Rayleigh waves, the inverse problem is solved to evaluate the elastic properties of the tested concrete. The inversion of Lamb waves involves modeling of the slab by assuming a thickness (if not known), a Poisson's ratio and a shear wave velocity. Therefore, the modal Lamb wave solution is calculated using Lamb wave theory, then compared to the experimental modes. If the calculated solution does not match the experimental one, the model is adjusted and a new Lamb wave modal solution is computed. The process is repeated until the theoretical solution agrees with the experimental modal curves. The final assumed model is then considered to be illustrative of the concrete slab properties. The inversion of Rayleigh waves is performed on the fundamental-mode using the

same modeling approach as in the inversion of the *SASW* data. If higher order modes of Rayleigh waves are identified, the theoretical modal solution is calculated for the layered system (profile) obtained from the inversion of the fundamental-mode, then the computed theoretical curves are compared to the experimental modes in order to verify the uniqueness of the solution. This leads to more accuracy in the estimation of concrete elastic properties with depth.

EXPERIMENTAL PROGRAM

Specimens

Two large concrete slabs, homogeneous and layered respectively, were tested in this study. The concrete slabs had identical dimensions of 3.5 m (11.5 ft) length, 3.0 m (9.8 ft) width and 0.8 m (2.6 ft) depth. Half the surface area of the homogeneous slab was longitudinally and transversally reinforced with 16 mm diameter (0.63 in.) steel bars (**Fig. 2**); spacing was 0.20 m (7.9 in.) and cover was 0.10 m (3.9 in.). The layered slab consisted of three layers with different elastic properties of concrete increasing from the top layer to the bottom layer. The thicknesses of concrete layers were varied in the longitudinal direction of the slab as shown in **Fig. 3**. Cylinders of 100 × 200 mm (3.9 × 7.9 in.) dimensions were made from the same batches of the different mixtures for mechanical testing. The mixtures used for the fabrication of the concrete slabs were prepared using a maximum aggregate size of 20 mm (0.8 in.) and 5% entrained air. The measured mass densities, compressive strengths, Young's moduli and Poisson's ratios of all mixtures are listed in **Table 1**.

Items of Investigation

The experiments on the homogeneous concrete slab were carried out in order to examine the accuracy of the *FK* method to determine Poisson's ratio and Young's modulus of concrete

slabs. The effect of reinforcement bars on *FK* measurements was also studied on this slab. The second goal of the experimental work was to investigate the potential of the *FK* method to detect and characterize concrete layering; this element was studied on the layered slab.

Testing

FK measurements were taken on four parallel lines (L1, L2, L3 and L4) at the free surface of each slab in the transversal direction as illustrated in **Fig. 4**. The tests carried out at the free surface of the homogeneous slab were accomplished using a 50 kHz piezoelectric accelerometer and a pulsar 50 kHz source to generate waves in twelve (12) different positions. The distance between each two consecutive positions of the source was 0.15 m (5.9 in.). The source was placed at 0.45 m (17.7 in.) from the first position of the accelerometer, which was located at 0.50 m (19.7 in.) from the edge of the slab. Good contact between the transducers (source, accelerometer) and the concrete surface was established using Vaseline coupling. The acquisition parameters were adjusted to attenuate body waves and ensure a significant amount of Lamb and Rayleigh wave energy in the record. The equipment used for this purpose was a two-channel (2) portable data acquisition system. The signals were acquired at a sampling frequency of 500 kHz and a total duration time of 4096 μ sec.

The measurements on the layered slab were conducted using a series of five (5) accelerometers (type 4396-B&K, 49 kHz natural frequency) and a steel ball source of 8 mm (0.3 in.) diameter. The spacing between adjacent accelerometers was 0.04 m (1.6 in.), and the impact was produced at six (6) different positions of the source. The distance between each two consecutive positions was 0.20 m (7.9 in.) and the source was initially placed at 0.20 m (7.9 in.) from the first accelerometer in the series. At the end of the test, thirty (30) signals

were collected on each measurement line at a sampling frequency of 200 kHz, and a total duration time of 1024 μsec .

EXPERIMENTAL RESULTS AND DISCUSSION

Assessment of Concrete Quality

The seismogram collected at the free surface of the homogeneous slab, on the measurement line L1, is presented in **Fig. 5** with the corresponding *FK* image (contour plot of energy). The image demonstrates high energy of Lamb waves in the concrete slab. The dispersion curves determined by selecting the peaks of energy on the *FK* image are shown in **Fig. 6(a)**. The shear wave velocity (V_S) in concrete was directly determined as the value to which tends Lamb wave higher order modes at high frequencies²⁰; it was evaluated to 2430 m/s (7,972 ft/s). The fundamental-mode of Rayleigh waves (R_f) was identified as the superposition of the symmetrical (S_f) and the antisymmetrical (A_f) fundamental-modes of Lamb waves¹⁶; this phenomenon was observed at frequencies higher than 5 kHz. The identified Rayleigh waves show constant phase velocity (V_R) equal to 2225 m/s (7,300 ft/s) for all frequencies. This occurs only in homogeneous media (i.e. not layered) and it demonstrates identical concrete quality in terms of depth. The Poisson's ratio (ν) of concrete was thus determined using the following approximate formula¹⁶:

$$\nu = \frac{V_R - 0.87 V_S}{1.12 V_S - V_R} \quad (1)$$

This formula can be used only for homogeneous media where Rayleigh waves are not dispersive, i.e. the different frequencies propagate with a constant phase velocity. The calculation led to a Poisson's ratio equal to 0.22, which is very close to 0.215 the mean measured value by mechanical testing on the concrete cylinders. The pressure wave velocity (V_P) in concrete was estimated as follows:

$$V_P = \sqrt{\frac{2(1-\nu)}{1-2\nu}} \times V_S \quad (2)$$

$$V_P = \sqrt{\frac{2(1-0.22)}{1-2 \times 0.22}} \times 2430 = 4056 \text{ m/s (13,307 ft/s)}$$

which indicates a concrete quality “generally good” according to the classification of Whitehurst²¹. The theoretical Lamb wave solution was computed using the evaluated shear wave velocity, the calculated Poisson’s ratio and the known thickness of the slab (0.80 m [2.6 ft]). The resulting symmetrical and antisymmetrical modes were overlaid on the *FK* image and compared to the experimental Lamb wave modes to verify the exactness of the evaluated parameters. A good agreement was observed between the theoretical and the experimental dispersion curves determined by selecting the crests of energies on the *FK* image. This indicates that the estimated properties of the concrete slab are reliable and there is no need to adjust the shear wave velocity or the Poisson’s ratio in additional iterations. Thereafter, the concrete Young’s modulus (E) was calculated using the mass density (ρ) obtained by physical characterization of the concrete cylinders (in case this parameter is unknown, a reasonable value of 2400 or 2500 kg/m³ (150 or 156 lb/ft³) can be assumed without significantly affecting the result), the estimated shear wave velocity and the calculated Poisson’s ratio:

$$E = 2 \rho \times (1 + \nu) \times V_S^2 \quad (3)$$

$$E = 2 \times 2354 \times (1 + 0.22) \times 2430^2 = 33.9 \text{ GPa (4,920,000 psi)}$$

This value matches very well the Young’s modulus of 35.1 GPa (5,090,000 psi) measured by mechanical testing with a relative difference less than 4%. The same results were obtained on the other measurement lines. The **Fig. 6** shows the experimental dispersion curves measured on the four (4) measurement lines with the theoretical Lamb wave solution calculated for the concrete slab (thickness = 0.80 m [2.6 ft], shear wave velocity = 2430 m/s [7,972 ft/s],

Poisson's ratio = 0.22); it reveals repeatability of *FK* results and identical concrete quality under all the measurement lines.

Effect of reinforcement bars on *FK* measurement

In order to examine the effect of reinforcement bars on *FK* measurement, the seismogram collected on the measurement line L2 in the non-reinforced region of the homogeneous concrete slab was compared to that collected on the measurement line L3 in the reinforced region of the slab. The comparison shows additional oscillations in the signals of the measurement line L3 after the first arrivals as illustrated in **Fig. 7**. The pulse energy generated by the piezoelectric source at these measurement lines was constant. Moreover, the measurement lines L2 and L3 have identical reflecting geometries, because they are located at the same distances from the reflecting edges of the slab. Therefore, the difference between the signal's amplitudes in the two seismograms, which illustrates the observed oscillations, corresponds only to the effect of the reinforcement bars. Similar effects were revealed on the seismogram of the measurement line L4 (reinforced region) when compared to that of the measurement line L1 (non-reinforced region). This result supports those obtained in the numerical study of Wu et al.²², which demonstrated that the existence of steel reinforcement bars in concrete causes a certain amount of the elastic energy generated to bounce back and forth between the concrete surface and the steel bars. This energy is primarily dependent on the steel bars diameter, the cover thickness and the spacing between the reinforcement bars. The study also mentions that the reflections from adjacent steel bars are added together to create long signal oscillations after the first arrivals. However, the observed effect of reinforcement bars (additional oscillations) did not influence the final *FK* results; **Fig. 6** shows identical dispersion curves for the *FK* tests conducted in the non-reinforced region of the concrete slab (L2 and L3) and those in the reinforced region of the slab (L3 and L4).

Assessment of Concrete Layering

The data recorded at the free surface of the layered slab, on the L1 measurement line, are presented in **Fig. 8** with the corresponding *FK* image. The Lamb wave modes selected on the image are shown in **Fig. 9**. The shear wave velocity was evaluated to approximately 2430 m/s in the same manner as that used for the homogeneous slab. The theoretical Lamb wave solution was computed using the known thickness of the slab, the evaluated shear wave velocity and an assumed Poisson's ratio. This last parameter was adjusted until the calculated theoretical curves matched the experimental results; the final assumed value was 0.22. A Young's modulus equal to 34.0 GPa (4,931,000 psi) was evaluated for this slab using equation (3); the mass density used for the calculation was taken equal to 2364 kg/m³ (147.6 lb/ft³) which is the mass density of all layers averaged proportionally to their thicknesses. The comparison between the estimated Young's modulus (34.0 GPa, [4,931,000 psi]) and the average measured Young's moduli of all layers proportionally to their thickness ($27.3 \times \frac{0.16}{0.8} + 29.6 \times \frac{0.08}{0.8} + 35.4 \times \frac{0.56}{0.8} = 33.2$ GPa [4,815,000 psi]) shows reliable estimation with a relative difference less than 3%. Note that the evaluated shear wave velocity, Poisson's ratio and Young's modulus are global characteristics of the layered slab and they are not related to a specific layer.

The superposition of Lamb wave fundamental-modes (A_f) and (S_f), which illustrates the fundamental-mode of Rayleigh waves (R_f), was observed at frequencies higher than 5 kHz. The identified Rayleigh waves were extracted and their phase velocity was plotted versus the wavelength, as illustrated in **Fig. 10(a)**. Presenting Rayleigh wave phase velocity in terms of wavelength instead of frequency aims to a better reading of the result; in general, a change in phase velocity that occurs at a given wavelength indicates a change in material properties (variation in shear wave velocity) at a depth approximately equal to half of the wavelength.

The obtained dispersion curve corresponds to the fundamental-mode of Rayleigh waves; its phase velocity varies between 2100 m/s (6,890 ft/s) and 2200 m/s (7,218 ft/s) from short wavelengths to long wavelengths. This variation symbolizes the dispersion of Rayleigh waves and thus denotes layering into the concrete slab. Rayleigh wave phase velocity depends on the concrete Young's modulus more than its compressive strength; this explains the small increase in Rayleigh wave phase velocity (100 m/s, [328 ft/s]) and attributes it to the fact that Young's moduli of the concrete layers are relatively close. The evaluated dispersion curve demonstrates that Rayleigh waves were formed up to a maximum wavelength of 0.46 m (18.1 in.). This indicates a maximum investigation depth of approximately 0.23 m (9 in.), which generally corresponds to half of the greatest wavelength involved in the *FK* test¹¹; therefore, only the first layer of the concrete slab can be detected. The inversion of the Rayleigh wave dispersion curve was thus performed by modeling the concrete as a system of five (5) layers having a total thickness of 0.23 m (9 in.). Equal thicknesses of 0.04 m (1.6 in.) were assumed for the first four (4) layers, while the thickness of the last layer was taken to be 0.07 m (2.8 in.). A shear wave velocity of 2300 m/s (7,546 ft/s) was affected for the five layers of the system in the initial model. The Poisson's ratio and the mass density were taken equal to those measured on the cylinders. In general, the Poisson's ratio and the mass density of concrete are unknown and reasonable values of these parameters (for example: Poisson's ratio = 0.21 and mass density = 2400 kg/m³ [150 lb/ft³]) can be assumed for all layers in the initial model without significantly changing the final result of the inversion. The effect of mass density on the evaluation of the theoretical dispersion curve (which is compared to the experimental data) is always negligible³, while that of Poisson's ratio was found to be insignificant (variation in the calculated phase velocity less than 2.5 % for a Poisson's ratio varying between 0.15 and 0.25 in the model). The shear wave velocity always has the greatest effect, and thus it is the only parameter that was adjusted in the model during the inversion process. The final computed

(theoretical) dispersion curve matching the experimental data is presented in **Fig. 10(a)**; a good agreement indicating exactness of the inversion is observed between the experimental and the theoretical dispersion curves. The corresponding model (final assumed shear wave velocity profile) obtained at the end of the inversion is presented in **Fig. 10(b)**; it clearly shows the top layer of the concrete slab with a thickness of 0.16 m and a mean shear wave velocity equal to 2332 m/s (7,651 ft/s). It also shows the middle layer of the concrete slab where a stronger shear wave velocity of 2520 m/s (8,268 ft/s) is observed. The evaluated shear wave velocities indicate good concrete quality in the top and the middle layers of the slab. The Young's modulus profile was determined using equation (3) and presented in Fig. 10(c). A relative difference of 15% was observed between the estimated Young's modulus profile and the values measured on the concrete cylinders. Similar results were obtained on the other measurement lines; the top layer of the concrete slab was detected and its thickness was accurately investigated.

CONCLUSIONS

This paper investigated the applicability of using Lamb guided waves and Rayleigh surface waves to nondestructively characterize concrete slabs. Multi-sensor tests were performed at the surfaces of two concrete slabs to evaluate concrete quality and layering. Based on the experimental results, the following conclusions can be drawn:

1. The proposed methodology of analysis of Lamb and Rayleigh waves offers a tool with great potential to resolve the modal propagation problem of these waves in concrete and thus investigate its elastic properties; Young's modulus and Poisson's ratio of concrete slabs can be accurately evaluated by using the multi-sensor approach presented in this paper; the test setup is simple and requires access to only one surface of the concrete slab.

2. The influence of reinforcement bars on the results of Lamb and Rayleigh wave testing is negligible for the bar size, cover and spacing used in this study; greater cover and spacing should not affect the final results of investigation.
3. Layering can be detected in concrete; the material quality and thickness of each layer can be estimated from the obtained shear wave velocity profile up to a maximum depth approximately equal to one quarter of the slab thickness.
4. The experimental results reported in this study were in good agreement with the theoretical values and matched the concrete properties very well. However, statistical calculations of uncertainty related to data collection, *FK* analysis and inversion are suggested for further research.
5. The non-intrusive multi-sensor method presented in this paper can be fully automated and easily used on full-scale concrete structures. It is mainly proposed for the inspection of concrete slabs when investigation is needed to verify concrete quality and integrity between the existing layers. The method is also suggested for the detection of near surface damage in concrete structures (dams, tunnels) and the determination of the depth of deterioration prior to repair operations.

ACKNOWLEDGMENTS

This work was supported by Hydro-Québec, the Natural Sciences and Engineering Research Council (NSERC)-Industry Research Chair on concrete NDT and instrumentation, and the University of Sherbrooke. The authors especially thank Stephane Tremblay and Martin Lizotte (Research Institute of Hydro-Québec), Danick Charbonneau (University of Sherbrooke) for their technical involvement in this research work. The help of Shahid Kabir in going over the English in the manuscript is greatly appreciated. Thanks are also addressed to Dr. David Hubble, Dr. Syed Imran and Dr. Zoubir Lounis from National Research Council Canada,

Institute for Research in Construction for their help in reviewing the final version of the manuscript.

NOTATION

Na = number of accelerometers

dx = spacing between each couple of accelerometers

d = distance between the source and the nearest accelerometer

Np = number of positions of the source at the concrete surface

V_{ph} = phase velocity

f = frequency

k = wavenumber

V_P = pressure wave velocity

V_S = shear wave velocity

V_R = Rayleigh wave phase velocity

ν = Poisson's ratio

ρ = mass density

E = Young's modulus

A_f = antisymmetrical fundamental-mode of Lamb waves

A_i = antisymmetrical higher order modes of Lamb waves, $i = 1, 2, 3$, etc. is the mode order

S_f = symmetrical fundamental-mode of Lamb waves

S_i = symmetrical higher order modes of Lamb waves, $i = 1, 2, 3$, etc. is the mode order

R_f = fundamental-mode of Rayleigh waves

REFERENCES

1. Sansalone, M.J. and Streett, W.B., "Impact-echo, non-destructive evaluation of concrete and masonry," Bullbrier Press, Ithaca, N.Y., 1997.
2. Maierhofer, Ch., Wöstmann, J., Krause, M., Milmann, B., Behrendt B., "Non-destructive characterisation of mortar layers for concrete repair using radar and ultrasonics," Proceedings of the International Symposium (NDT-CE 2003) Non-Destructive Testing in Civil Engineering 2003, Berlin, Germany, September 16-19, 2003.
3. Nazarian, S., "In situ determination of elastic moduli of soil deposits and pavement systems by Spectral Analysis of Surface Waves method," Ph.D. thesis, University of Texas at Austin, 1984.
4. Stokoe, K. H., Wright, S. G., Bay, J. A., and Roesset, J. M., "Characterization of geotechnical sites by SASW method," Proceedings of the Geophysical Characterization of Sites, ISSMFE Technical Committee 10, New Delhi, 1994.
5. Rix, G. J., and Leipski, E. A., "Accuracy and resolution of surface wave inversion," Recent Advances in Instrumentation, Data Acquisition and Testing of Soil Dynamics, ASCE Geotechnical Special Publication, No. 29, 1991, pp. 17-32.
6. Cho, Y. S., "NDT response of spectral analysis of surface wave method to multi layer thin high strength concrete structures," *Ultrasonics*, V. 40, 2002, pp. 227-230.
7. Kalinski, M. E., "Measurements of intact and cracked concrete structural elements by the SASW method," Master thesis, University of Texas at Austin, 1994.
8. Hassaim, M., Rhazi, J., Ballivy, G., and Khayat, K., "Évaluation de l'état du béton par la technique d'analyse spectrale des ondes de Rayleigh," *Canadian Journal of Civil Engineering*, V. 28, 2001, pp. 1018-1028.
9. Krstulovic-Opara, N., Woods, R. D., and Al-Shayea, N., "Nondestructive testing of concrete structures using the Rayleigh wave dispersion method," *ACI Materials Journal*, V.

93, No. 1, 1996, pp.75-86.

10. Bay, J. A., and Stokoe, K. H., "Field determination of stiffness and integrity of PCC slabs using the SASW method," Proceedings of the Conference on Nondestructive Evaluation of Civil Structures and Materials, 1990, pp 71-85.

11. Al Wardany, R., "Nondestructive characterization of concrete structures using Rayleigh and Lamb dispersive waves," Ph.D. thesis (in French), University of Sherbrooke, 2005.

12. Karray, M. and Lefebvre G., "Identification and isolation of multiple modes in Rayleigh waves testing Methods," Proceedings of the Use of Geophysical Methods in Construction, sessions of Geo-Denver, ASCE, Denver, Colorado, USA, August 2000, pp 80-94.

13. Tokimatsu, K., Tamura, S., and Kojima, H., "Effects of multiple modes on Rayleigh wave dispersion," *Journal of Geotechnical Engineering*, ASCE, V. 118, No. 10, 1992, pp. 1529-1543.

14. Lamb, H., "On waves in an elastic plate," Proceedings of the Royal Society of London, V.93, No. 651, 1917, pp. 293-312.

15. Rayleigh, L., "On waves propagated along the plane surface of an elastic solid," Proceedings of the London Mathematical Society, V. 17, London, 1885, pp. 4-11.

16. Viktorov, I. A., "Rayleigh and Lamb waves: physical theory and applications," Plenum Publishing Corporation, New York, 1967.

17. Foti, S., "Multi-station methods for geotechnical characterization using surface waves," Ph.D. thesis, Politecnico di Torino, 2000.

18. Gabriels, P., Snieder, R., and Nolet G., "In situ measurement of shear wave velocity in sediments with higher-mode Rayleigh waves," *Geophysical prospecting*, V. 35, 1987, pp. 187-196.

19. Al-Hunaidi M. O., "Nondestructive evaluation of pavements using spectral analysis of surface waves in the frequency wavenumber domain," *Journal of Nondestructive Evaluation*,

V. 15, No. 2, 1996, pp. 71-82.

20. Ryden, N., Park, C. B., Ulriksen, P., and Miller, R. D., "Multimodal approach to seismic pavement testing," *Journal of Geotechnical and Geoenvironmental Engineering*, V. 130, No. 6, 2004, pp. 636-645.

21. Whitehurst, E. A., "Soniscope tests concrete structures," *Journal of the American Concrete Institute*, V.47, No 6, 1951, pp. 433-444.

22. Wu, T. T., Sun, J. H., and Tong, J. J., "On the study of elastic wave scattering and Rayleigh wave velocity measurement of concrete with steel bar," *NDT&E International*, V. 33, 2000, pp. 401-407.

TABLES AND FIGURES

List of Tables:

Table 1–Material characteristics of the concrete mixtures

List of Figures:

Fig. 1–*FK* test setup.

Fig. 2–Longitudinal section of the homogeneous concrete slab.

Fig. 3–Longitudinal section of the Layered concrete slab.

Fig. 4– Measurement lines on the concrete slabs.

Fig. 5–**(a)** Seismogram acquired at the surface of the homogeneous concrete slab on the L1 measurement line; **(b)** corresponding *FK* image (contour plot of energy, darkest zones represent highest energy); theoretical Lamb wave modes matching the distribution of energy are overlaid (antisymmetrical modes: solid lines and symmetrical modes: dashed lines).

Fig. 6–Experimental Dispersion curves (circles) determined by selecting the peaks of energy on the *FK* images of the homogeneous concrete slab; theoretical Lamb wave modes matching the experimental data are overlaid (antisymmetrical modes: solid lines and symmetrical modes: dashed lines), **(a)**: measurement line L1; **(b)**: measurement line L2; **(c)**: measurement line L3; **(d)**: measurement line L4.

Fig. 7–Seismograms acquired in **(a)** the reinforced region of the homogeneous concrete slab on the L3 measurement line; **(b)** the non reinforced region of the homogeneous concrete slab on the L2 measurement line; **(c)** effect of reinforcement bars obtained from the difference between the two seismograms.

Fig. 8–**(a)** Seismogram acquired at the surface of the layered concrete slab on the L1 measurement line; **(b)** corresponding *FK* image (contour plot of energy, darkest zones

represent highest energy); theoretical Lamb wave modes matching the distribution of energy are overlaid (antisymmetrical modes: solid lines and symmetrical modes: dashed lines).

Fig. 9–Experimental Dispersion curves (circles) determined by selecting the peaks of energy on the *FK* image of the layered concrete slab (measurement line L1); theoretical Lamb wave modes matching the experimental data are overlaid (antisymmetrical modes: solid lines and symmetrical modes: dashed lines); Rayleigh waves are identified.

Fig. 10–(a) Experimental dispersion curve of Rayleigh waves obtained on the measurement line L1 of the layered concrete slab; theoretical Rayleigh wave fundamental-mode matching the experimental data is overlaid; (b) corresponding shear wave velocity profile obtained by inversion (final model); (c) calculated Young’s modulus profile compared to the result of mechanical testing.

Table 1–Material characteristics of the concrete mixtures

Slab	Cylinder	Mass density, kg/m ³ (lb/ft ³)	Compressive strength, MPa (psi)	Young’s modulus, GPa (psi)	Poisson’s ratio	
Homogeneous	1	NM	39.8 (5,772)	NM	NM	
	2	2360 (147)	40.9 (5,932)	35.7 (5,177,847)	0.22	
	3	2348 (146)	40.3 (5,845)	34.4 (4,989,298)	0.21	
	<i>Mean</i>	<i>2354 (147)</i>	<i>40.3 (5,845)</i>	<i>35.1 (5,090,824)</i>	<i>0.22</i>	
Layered	Top layer	1	NM	17.6 (2,553)	NM	NM
		2	2378 (148)	17.1 (2,480)	27.5 (3,988,537)	0.22
		3	2383 (149)	17.3 (2,509)	27.1 (3,930,523)	0.20
		<i>Mean</i>	<i>2380 (149)</i>	<i>17.3 (2,509)</i>	<i>27.3 (3,959,530)</i>	<i>0.21</i>
	Middle layer	1	NM	30.2 (4,380)	NM	NM
		2	2311 (144)	27.6 (4,003)	29.6 (4,293,117)	0.14
		3	2343 (146)	27.7 (4,017)	29.6 (4,293,117)	0.16
		<i>Mean</i>	<i>2327 (145)</i>	<i>28.5 (4,133)</i>	<i>29.6 (4,293,117)</i>	<i>0.15</i>
	Bottom layer	1	NM	39.5 (5,729)	NM	NM
		2	2354 (147)	37.9 (5,497)	34.3 (4,974,794)	0.19
		3	2375 (148)	34.6 (5,018)	36.4 (5,279,374)	NM
		<i>Mean</i>	<i>2365 (148)</i>	<i>37.3 (5,410)</i>	<i>35.4 (5,134,336)</i>	<i>0.19</i>

*NM : Not Measured

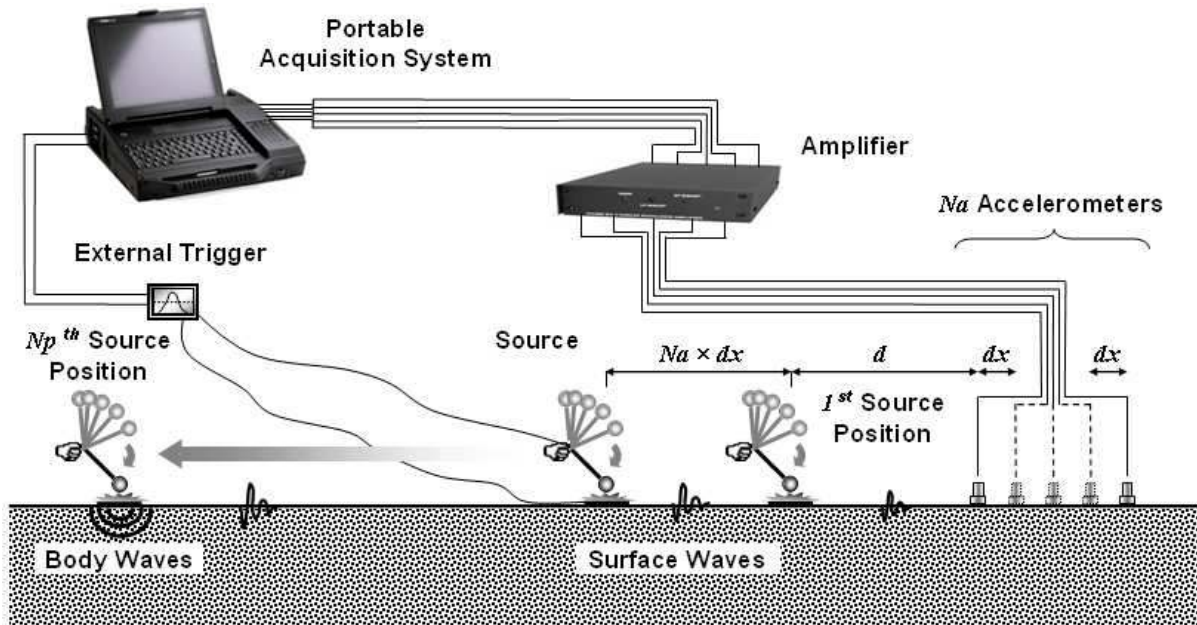


Fig. 1–FK test setup.

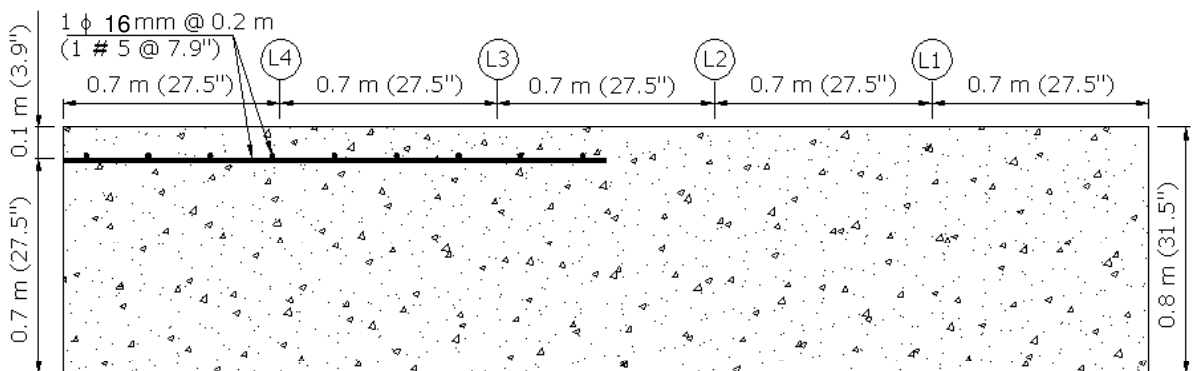


Fig. 2–Longitudinal section of the homogeneous concrete slab.

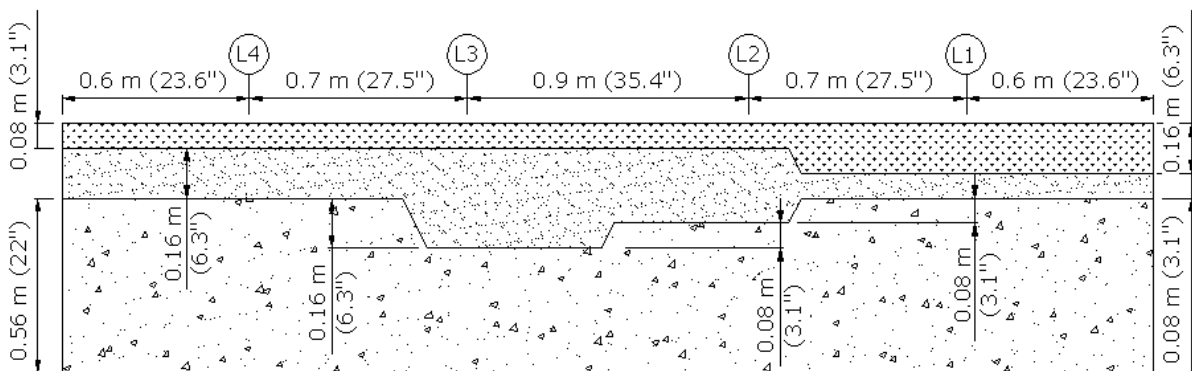


Fig. 3–Longitudinal section of the Layered concrete slab.

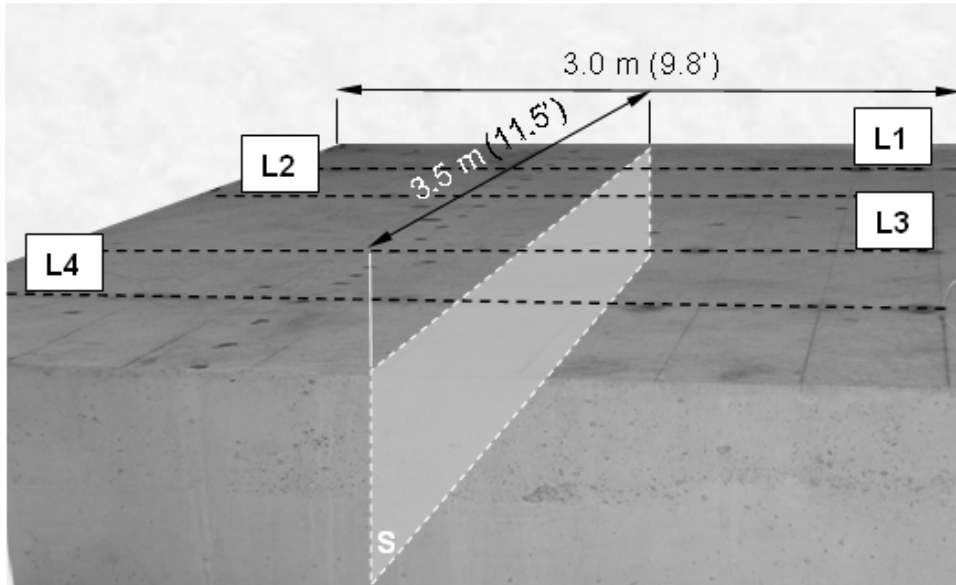


Fig. 4– Measurement lines on the concrete slabs.

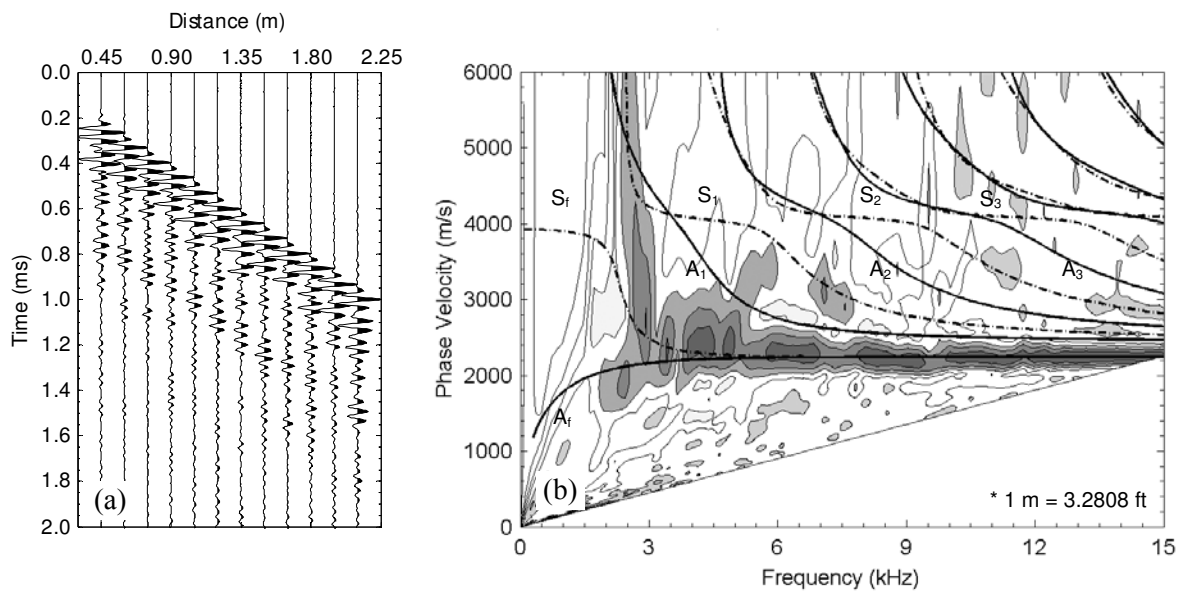


Fig. 5–(a) Seismogram acquired at the surface of the homogeneous concrete slab on the L1 measurement line; (b) corresponding *FK* image (contour plot of energy, darkest zones represent highest energy); theoretical Lamb wave modes matching the distribution of energy are overlaid (antisymmetrical modes: solid lines and symmetrical modes: dashed lines).

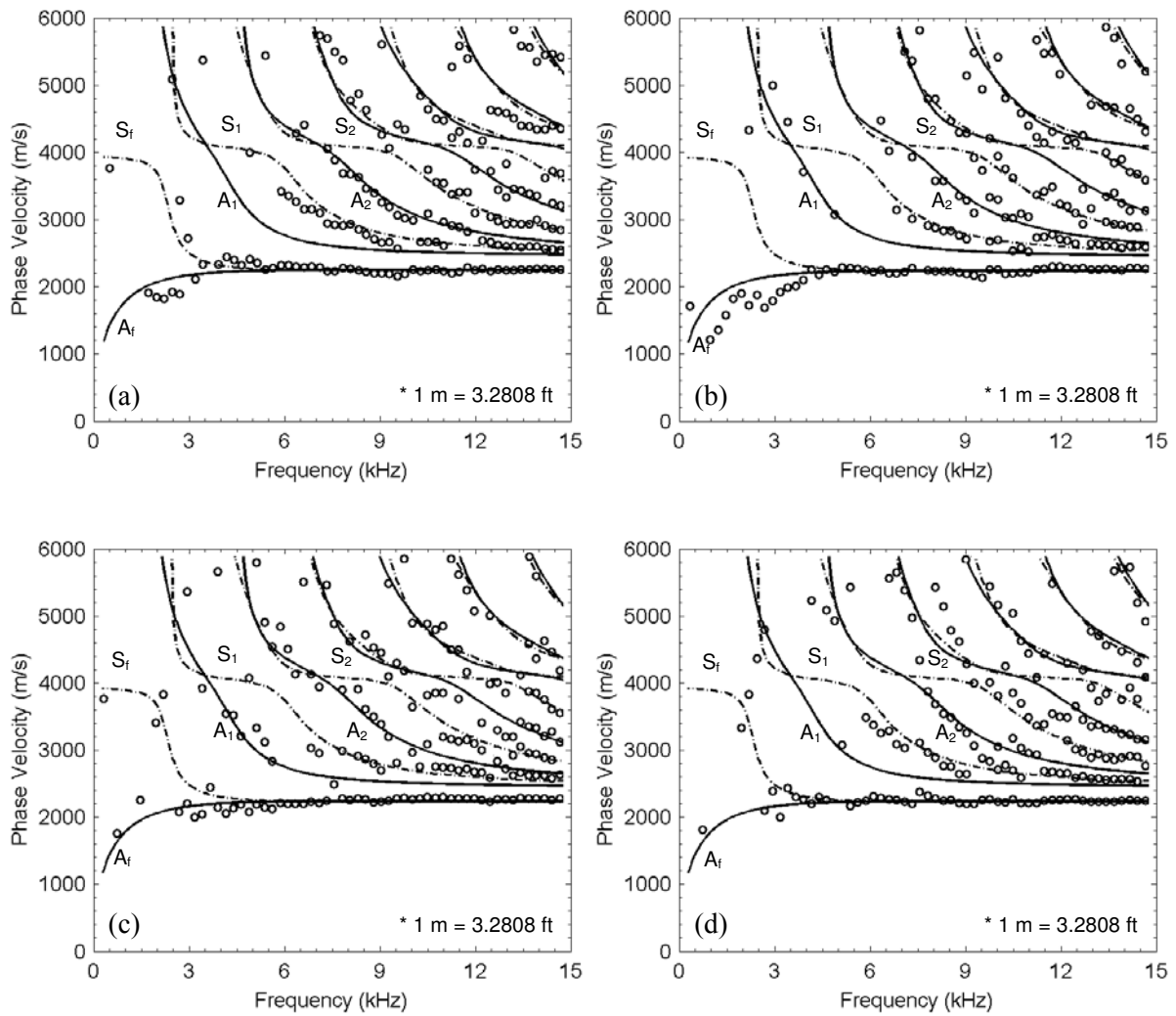


Fig. 6—Experimental Dispersion curves (circles) determined by selecting the peaks of energy on the *FK* images of the homogeneous concrete slab; theoretical Lamb wave modes matching the experimental data are overlaid (antisymmetrical modes: solid lines and symmetrical modes: dashed lines), (a): measurement line L1; (b): measurement line L2; (c): measurement line L3; (d): measurement line L4.

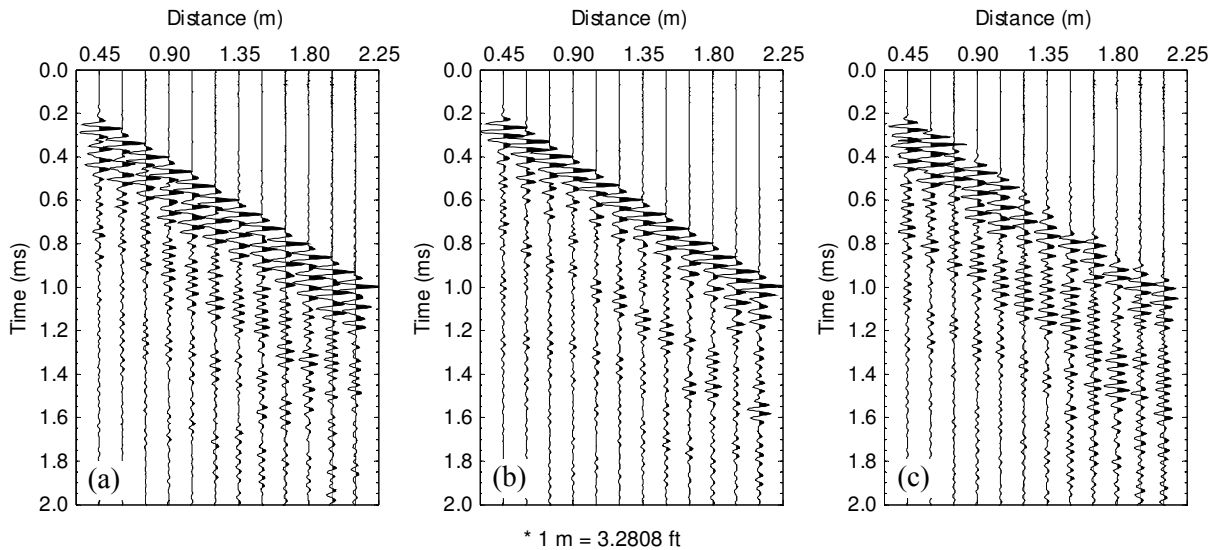


Fig. 7–Seismogram acquired in (a) the reinforced region of the homogeneous concrete slab on the L3 measurement line; (b) the non reinforced region of the homogeneous concrete slab on the L2 measurement line; (c) effect of reinforcement bars obtained from the difference between the two seismograms.

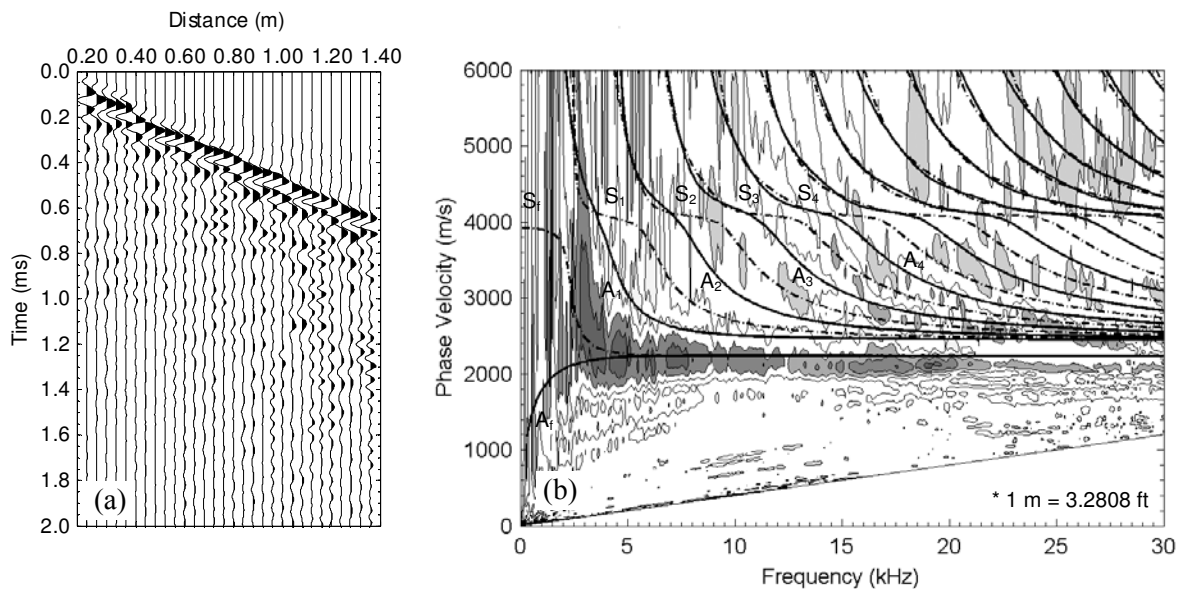


Fig. 8–(a) Seismogram acquired at the surface of the layered concrete slab on the L1 measurement line; (b) corresponding *FK* image (contour plot of energy, darkest zones represent highest energy); theoretical Lamb wave modes matching the distribution of energy are overlaid (antisymmetrical modes: solid lines and symmetrical modes: dashed lines).

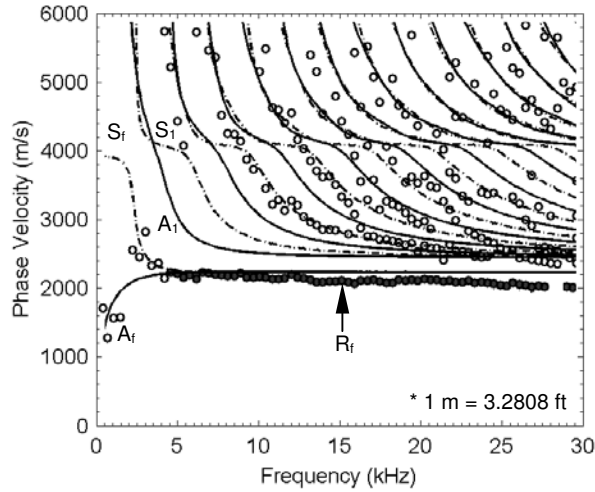
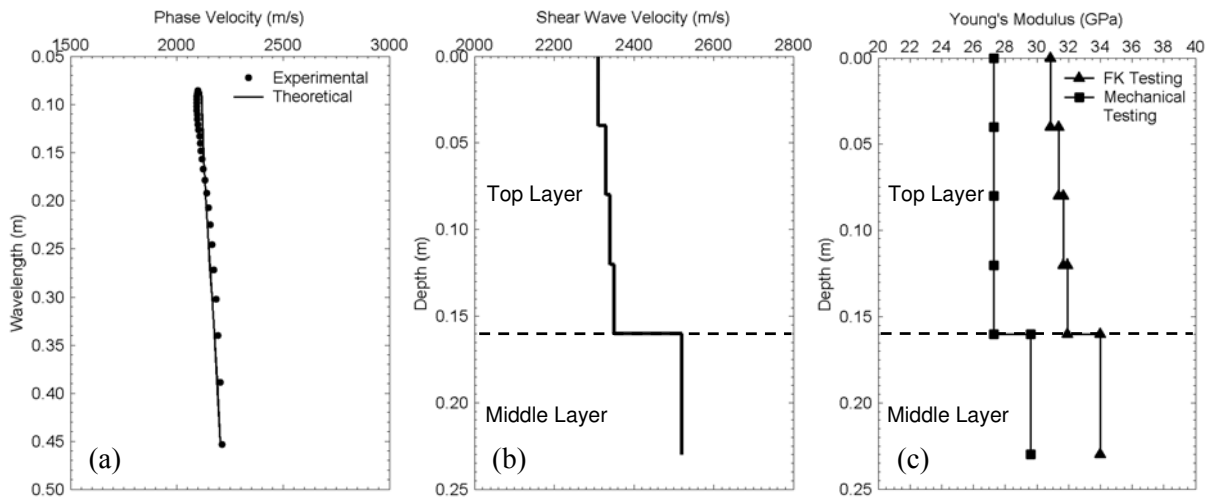


Fig. 9–Experimental Dispersion curves (circles) determined by selecting the peaks of energy on the *FK* image of the layered concrete slab (measurement line L1); theoretical Lamb wave modes matching the experimental data are overlaid (antisymmetrical modes: solid lines and symmetrical modes: dashed lines); Rayleigh waves are identified.



* 1 m = 3.2808 ft, 1 GPa = 145,037.7 psi

Fig. 10–(a) Experimental dispersion curve of Rayleigh waves obtained on the measurement line L1 of the layered concrete slab; theoretical Rayleigh wave fundamental-mode matching the experimental data is overlaid; (b) corresponding shear wave velocity profile obtained by inversion (final model); (c) calculated Young's modulus profile compared to the result of mechanical testing.